



DR. JING ZHANG (Orcid ID : 0000-0002-7290-8304)

MS. LITING LI (Orcid ID : 0000-0003-1165-4360)

MS. MEIHONG ZHANG (Orcid ID : 0000-0001-9656-7180)

Article type : Original Articles

Handling Editor: Emma Andersson

Title:

**Low-GGT intrahepatic cholestasis associated with biallelic *USP53* variants:
clinical, histological, and ultrastructural characterization**

Jing Zhang,^{1,2#} Ye Yang,^{1,2#} Jing-Yu Gong,¹ Li-Ting Li,² Jia-Qi Li,¹ Mei-Hong Zhang,¹ Yi Lu,²
Xin-Bao Xie,² Yu-Ren Hong,³ Zhang Yu,³ A. S. Knisely,⁴ Jian-She Wang^{2*}

Affiliations:

¹ The Department of Pediatrics, Jinshan Hospital, Fudan University, Shanghai 201508, China

² The Center for Pediatric Liver Diseases, Children's Hospital of Fudan University; Department of Pediatrics, Shanghai Medical College of Fudan University, Shanghai 201102, China

³ Electron Microscopy Core Laboratory, Shanghai Medical College, Fudan University, Shanghai 200032, China

⁴ Institut für Pathologie, Medizinische Universität Graz, 8010 Graz, Austria

These authors contributed equally to this work.

***Corresponding Author:**

Jian-She Wang, M.D., Ph.D.

The Center for Pediatric Liver Diseases,
Children's Hospital of Fudan University,

This article has been accepted for publication and undergone full peer review but has not been through the copyediting, typesetting, pagination and proofreading process, which may lead to differences between this version and the [Version of Record](#). Please cite this article as [doi: 10.1111/LIV.14422](https://doi.org/10.1111/LIV.14422)

This article is protected by copyright. All rights reserved

No. 399 Wanyuan Road, Minhang District,
Shanghai 201102, China
E-mail: jshwang@shmu.edu.cn; Tel: +86 21 64931171

Disclosure

The authors declare no conflicts of interest.

Author contributions

Jian-She Wang: Substantial contributions to the conception and design of the work; the acquisition, analysis, and interpretation of data for the work; drafting the work and revising it critically for important intellectual content;

Jing Zhang and Ye Yang: Substantial contributions to the experiment, analysis and interpretation of data for the work; writing the manuscript;

Jia-Qi Li: Substantial contributions to analysis and interpretation of exome sequencing for the work;

Mei-Hong Zhang, Yi Lu, Xin-Bao Xie: Substantial contributions to provide clinical information for the work;

Yu-Ren Hong and Zhang Yu: Contributions to transmission electron microscopy.

A. S. Knisely: Histopathologic evaluation; interpretation of clinical and histopathologic data; critical revision of the manuscript.

Financial support:

This project was funded by the National Natural Science Foundation of China, Grant Numbers 81570468 and 81873543 (to Jian-She Wang)

Abbreviations:

GGT: gamma-glutamyltransferase

WES: whole-exome sequencing

CMV: cytomegalovirus

DB: direct bilirubin

TB: total bilirubin

TJP2: tight junction protein 2

CLDN1: claudin-1

TEOAE: transient evoked otoacoustic emission

ABR: auditory brainstem response

ASSR: auditory steady state response

PPV: predictedly pathogenic variants

USP53: ubiquitin carboxyl-terminal hydrolase 53

Lay Summary

To seek new genes implicated in pediatric hepatobiliary disease, we studied 69 Chinese children with jaundice of unknown cause. In 7 of them, all unrelated, gene sequencing found mutations in *USP53*, indicating that *USP53* is necessary for liver health. Some of our patients with *USP53* disease had hearing problems as well as jaundice. Their jaundice, however, responded well to medical treatment.

Abstract

Background and Aims: In about 20% of children with cholestasis and normal or low serum gamma-glutamyltransferase (GGT) activity, no etiology is identified. We sought new genes implicated in pediatric hepatobiliary disease.

Methods: We conducted whole exome sequencing in 69 children evaluated at our center from 2011 to 2018 who had low-GGT cholestasis and in whom homozygous / compound heterozygous predictedly pathogenic variants (PPV) in *ATP8B1*, *ABCB11*, *NR1H4*, *MYO5B*, or *TJP2* were not found. Clinical records and findings on light microscopy and transmission electron microscopy of liver-biopsy materials were reviewed.

Results: In 7 patients from 7 unrelated families, biallelic PPV (10 in total) were found in *USP53*, recently associated with intrahepatic cholestasis. Seven variants were classified as pathogenic: one canonical splicing, c.569+2T>C, and six nonsense or frameshifting: c.169C>T (p.Arg57Ter), c.581delA (p.Arg195GlufsTer38), c.831_832insAG (p.Val279GlufsTer16), c.1012C>T (p.Arg338Ter), c.1426C>T (p.Arg476Ter), and c.1558C>T (p.Arg520Ter). Three were likely pathogenic: c.297G>T (p.Arg99Ser), c.395A>G (p.His132Arg), and c.878G>T (p.Gly293Val). In all patients, jaundice began at age <7mo. Cholestasis was transient, with documented resolution of hyperbilirubinemia in all (oldest patient now aged 5y) except one, who was lost to follow-up. Light microscopy identified intralobular cholestasis, giant-cell change of hepatocytes, and perisinusoidal-perihepatocytic and portal-tract fibrosis. Ultrastructural study revealed elongated hepatocyte-hepatocyte tight junctions. One patient was deaf.

Conclusion: *USP53* interacts with the tight-junction constituent *TJP2*. *TJP2* mutation can cause low-GGT intrahepatic cholestasis, with elongated hepatocyte-hepatocyte tight junctions, as well as deafness. Our findings extend a preliminary report of *USP53* disease and indicate that *USP53* mutation may generate a partial phenocopy of *TJP2* disease. (250 words)

Keywords: low gamma-glutamyl transferase cholestasis, *TJP2*, transmission electron microscopy, deafness, *USP53*

Introduction

Genetic variants can explain normal or low serum γ -glutamyl-transferase (GGT) cholestasis in only 75% ~ 80% of pediatric patients.¹ Whole-exome sequencing (WES) has identified several genes implicated in low-GGT cholestasis, including *USP53*, encoding a protein of uncertain function that associates with cell-cell tight junctions, which was mutated in one family with cholestasis and hearing loss.² We independently used WES to identify *USP53* as mutated in 7 children with low-GGT intrahepatic cholestasis from 7 non-related families. We describe our WES studies and the mutations found, with clinical, histological, and ultrastructural features of

USP53 disease in these children.

Subjects and Methods

Ethical considerations

The study was approved by the ethics committees of Jinshan Hospital of Fudan University and Children's Hospital of Fudan University (both Shanghai, China), and was in accordance with the guidelines of the 1975 Declaration of Helsinki. Informed consent was obtained from parents of each child.

Subjects

Sixty-nine patients were enrolled in this study using a reported protocol.³ All were Chinese nationals (68 of Han ethnicity, one of paternal Manchu and maternal Han ethnicity); all were referred to a participating hospital from 2011 through 2018. We first excluded those patients with disease reasonably attributed to infection, drug exposure, autoimmune hepatitis, and biliary atresia. Cytomegalovirus (CMV) infection was not excluded due to its high prevalence in Chinese infants. The criteria for enrolment were: 1) direct bilirubin (DB) >20% of total bilirubin (TB) if TB >5 mg/dL, or DB >1 mg/dL if TB < 5mg/dL,⁴ and remarkably elevated total bile acids with no identified etiology of hepatobiliary disease; 2) low serum GGT values (defined as highest GGT <100 IU/L); 3) without identified pathological variants in *ATP8B1*, *ABCB11*, *NR1H4*, *TJP2*, and *MYO5B*, genes implicated in low-GGT intrahepatic cholestasis.⁵ Another 2 cohorts of children – “other-liver-disease” (unexplained high-GGT cholestasis, transaminitis, or liver cirrhosis, n=84) and “non-liver-disease” (n=1000) – who underwent WES on the same platform were used as controls.

Genetic analysis

Genomic DNA was extracted (QIAamp DNA Blood Mini Kit, 51106, Qiagen, Hilden, Germany) from peripheral blood of patients and of available family members (parents and siblings). WES was performed and annotation was done in the patient cohort and the 2 control groups as described (Genesky Biotechnologies, Shanghai, China).³ Total WES depth was 100 ×. WES data were analyzed following routine screening for candidate variants. Briefly, to be considered candidate gene variants, the criteria to be met were: 1) allele frequency < 0.01 in both the 1000 Genomes Project (1000G, <http://www.internationalgenome.org/data>) and the Exome Aggregation

Consortium Browser (ExAC, <http://exac.broadinstitute.org>); 2) variants leading to a premature stop codon, frameshifting, or located at a canonical splicing site, or predicted to be pathogenic by at least one of the 3 following programs: MutationTaster (<http://www.mutationtaster.org/>);⁶ Polymorphism Phenotyping v2 (Polyphen-2; <http://genetics.bwh.harvard.edu/pph2/index.shtml>),⁷ and Sorting Tolerant From Intolerant (SIFT; <http://sift.jcvi.org>);⁸ and 3) when biallelic, present only in low-GGT cholestasis patients. Targeted PCR was conducted in all 7 families according to the kit manufacturer's protocols (2× Master Mix KT201; Tiangen, Shanghai, China). Sanger sequencing was conducted to identify the origin of mutations (primers available on request). NM_019050.2 was used as the reference sequence for *USP53*.

Histologic and immunohistochemical studies of liver

Liver-biopsy specimens from *USP53* patients P3, P4, P6, and P7, obtained at ages 10mo8d, 10mo2d, 9mo20d, and 9mo7d respectively, were routinely formalin-fixed and paraffin-processed. Tissue sections at 4 μm were stained with hematoxylin and eosin and with Gömöri's reticulin technique. Sections also were immunostained, by standard techniques, with antibodies against *USP53* (HPA035844 and HPA 035845, 1:1000 dilution; Sigma-Aldrich, Taufkirchen, Germany),⁹ as well as against the tight-junction – associated antigens tight junction protein 2 (TJP2, LS-B2185, 1:100 dilution; LifeSpan BioScience, Seattle, WA) and claudin-1 (CLDN1, PA1-37464, ready-to-use; Invitrogen, Carlsbad, CA). Sections of a similarly processed liver-biopsy specimen from a child with cholestatic *TJP2* disease aged 11mo were used as a control. Histopathologic assessment by light microscopy was carried out without knowledge of patient clinical or genetic status.

Ultrastructure study

Transmission electron microscopy was done for P3 and P4 as described with small modifications.¹⁰ Liver biopsy materials were primarily fixed in 2.5% glutaraldehyde buffered in 0.2 M of phosphate buffer (pH 7.2) for 12 hours at 4°C and washed in 0.1 M of phosphate buffer (pH 7.2) three times (15 ~ 20min each time) before and after post-fixation in 1% osmium tetroxide for 2 hours at room temperature. They were dehydrated first in graded alcohols (50% ~ 90%), then in graded acetone (90% ~ 100%), and were embedded in epoxy resin. Ultra-thin sections were cut with a Leica EM UC7 ultramicrotome (Leica Microsystems, Wetzlar, Germany), mounted on copper grids, stained with uranyl acetate / lead citrate, and examined on a Zeiss EM 900 electron

microscope (Carl Zeiss, Vienna, Austria). Liver specimens from children with cholestatic *ATP8B1* and *ABCB11* disease were used as controls.

Auditory test

Routine hearing screening in the newborn by transient evoked otoacoustic emission (TEOAE) is a national program in China. For infants who fail initial testing, TEOAE is repeated at ages 1mo, 3mo, and 6 mo. If failure persists, further assessments – auditory brainstem response (ABR) and auditory steady state response (ASSR) testing – are performed.^{11,12} In ABR assessment, click stimuli at a rate of 27.7/s with high pass filter set at 100 Hz and low-pass filter at 2000 Hz are applied. A threshold of ≤ 30 dB nHL is regarded as hearing normal and a threshold of >70 dB nHL is regarded as severe hearing impairment (World Health Organization criteria for children, https://www.who.int/pbd/deafness/hearing_impairment_grades/en/). The highest level for tonal stimulus in ASSR is assigned as 120 dB nHL and a 4-frequency pure-tone-average threshold (0.5 kHz, 1 kHz, 2 kHz, 4 kHz) is calculated for each ear.

Statistical analysis

Statistical analyses were performed using software package STATA 10 (StataCorp, College Station, TX). Fisher's exact test was employed to compare the frequency of mutated alleles between the subjects and both "other-liver" controls and "non-liver" controls. Bilateral P values <0.05 were considered statistically significant.

Results

Biallelic pathogenic or predictedly pathogenic *USP53* variants: Association with low-GGT cholestasis

Among the 69 pediatric patients with low-GGT intrahepatic cholestasis who met our criteria, 7 patients from 7 unrelated families were identified as carrying biallelic *USP53* mutations in homozygous or compound-heterozygous form (Figure 1), in contrast to none in the "other-liver-disease" controls (7/69 vs. 0/84, $P=0.00319$) and none in the "non-liver-disease" controls (7/69 vs. 0/1000, $P=3.47e-9$). Autosomal recessive inheritance was confirmed by segregation of mutated alleles within pedigrees. Serum of all 7 patients was free from CMV DNA at the time of sampling. WES data in the 7 patients also excluded the possibility of other genes known to be associated

with low-GGT cholestasis (Supplementary Table S1).³ Although individual patients harbored variants in various other genes, those genes have no established relationships with liver disease (Supplementary Table S2).

Ten pathogenic or likely pathogenic variants (according to American College of Medical Genetics guidelines¹³), 2 known and 8 novel, in *USP53* were discovered in the 7 patients (Table 1). The 2 known variants were c.1012C>T (p.Arg338Ter) and c.1426C>T (p.Arg476Ter). Both of them are recorded in the ExAC database, but have not been described in association with disease. They are predicted to cause nonsense-mediated mRNA decay, and so are classified as pathogenic variants. Variant c.1012C>T was seen 5 times in our low-GGT cholestasis patients, significantly more frequently than in “other-liver-disease” controls (5/138 vs. 0/168, P=0.01792) and than in “non-liver-disease” controls (5/138 vs. 1/2000, P=5.95e-6).

The 8 novel variants included 5 that are pathogenic.¹³ One affected a canonical splicing site, c.569+2T>C, and 4 are predicted to lead to mRNA decay: c.169C>T (p.Arg57Ter); c.581delA (p.Arg195GlufsTer38); c.831_832insAG (p.Val279GlufsTer17); and c.1558C>T (p.Arg520Ter). Three are likely pathogenic¹³: c.297G>T (p.Arg99Ser); c.395A>G (p.His132Arg); and c.878G>T (p.Gly293Val). Each was detected once in the patients with low-GGT intrahepatic cholestasis. None was found in either of the control groups or in ExAC. Nonsense-mediated mRNA decay was demonstrated for the 3 variants c.581delA, c.1012C>T, and c.1558C>T (Supplementary Methods and Results, Supplementary Figure S1).

Clinical management and outcomes in 7 *USP53*-disease patients

All 7 children with biallelic *USP53* predictedly pathogenic variants (PPV) were born at term, with normal weight, following an uneventful pregnancy. All of them presented with jaundice when aged <7mo. No parental consanguinity was acknowledged. All were routinely managed with ursodeoxycholic acid (UDCA, 20mg/kg/d, divided into 2 doses daily) and fat-soluble vitamins. Cholestyramine (1g, once or twice daily) was administered to 5 patients when needed (Table 2). All patients except for P5 (lost to follow-up) at the time of this study were alive with their native liver (the oldest aged 5y), with serum total bilirubin levels normalized before age 2y. Transaminase activities in P2, P3, and P6 had returned to normal while slight elevations persisted in P1, P4, and P7 (Table 2). None has yet developed hepatocellular or cholangiocellular

malignancy.

Histopathologic, immunohistologic, and ultrastructural findings

Lobular disarray, hepatocellular cholestasis, and rosetting with canalicular cholestasis were seen in all 4 available liver samples (Figure 2). Giant-cell change of hepatocytes was seen in patients P3, P6, and P7, but not in P4. Fibrosis was obvious in all patients, with bridging fibrosis in P3, with perisinusoidal extension; perisinusoidal and pericellular fibrosis, with parenchymal nodularity, in P4; cirrhosis in P6; and portal-tract fibrosis and mixed acute and chronic inflammation in P7.

Immunostaining for USP53 was technically unsuccessful. However, expression and localization of 2 tight-junction – associated proteins, TJP2 and CLDN1, appeared both decreased and blurred (Supplementary Figure S2).

In the 2 *USP53*-disease patients from whom liver-biopsy material suitable for ultrastructural study was available (P3, P4), tight-junction complexes were elongated, extending from the bile-canalculus margin deeper into the intercellular space than was the case in patients with either *ATP8B1* disease or *ABCB11* disease (Figure 3).

Hearing disorders

Patient P6 failed TEOAE screening at ages 3d and 42d. A cochlear implant was placed at age 1y after failure in all assessments, including ABR (left ear, 97 dBnHL; right ear, 97 dBnHL) and ASSR (left ear, 115, 115, and 110 dBnHL and right ear, 65, 110, and 110 dBnHL at 500, 1000, and 2000 Hz respectively, with bilateral lack of response at 4000 Hz).

Patient P2 passed neonatal TEOAE screening. However, at age 1mo, he was noted not to respond to sounds. At age 4mo, ABR results in his right ear were slightly abnormal (35 dBnHL). Later he reacted to ambient sounds and at age 16mo and passed ABR re-assessment.

All other patients passed neonatal TEOAE screening and have shown no signs of hearing problems.

Discussion

A preliminary report, describing 3 Saudi children homozygous for *USP53* variant NM_019050.2:c.951delT, NP_061923.2:p.(Phe317LeufsTer6) within an extended family, proposed that mutation in *USP53* is associated with low-GGT cholestasis.² Our work, presenting 7 non-related patients with biallelic pathogenic or predictedly pathogenic variants in *USP53*, confirms and extends the genetic findings in that report; it also provides the first description of histopathologic and ultrastructural findings in the liver of patients with *USP53* disease.

USP53 encodes ubiquitin carboxyl-terminal hydrolase 53 (USP53), which belongs to the family of de-ubiquitinating enzymes. Lacking an essential histidine residue in the preserved catalytic domain, however, USP53 exhibits no deubiquitinase activity.¹⁴ In a mouse-deafness model,⁹ the homologous protein, *Usp53*, interacts with the tight-junction constituent tight junction protein 2 (*Tjp2*, encoded by *Tjp2*). Tight-junction associated proteins are involved in the survival of auditory hair cells and hearing, modulating the barrier properties and mechanical stability of tight junctions. Biallelic variants in *TJP2*, the human orthologue of *Tjp2*, cause hearing impairment^{15,16,17} and low-GGT intrahepatic cholestasis, with elongated hepatocyte-hepatocyte tight junctions.^{18,19} Reduced and blurred CLDN1 expression was observed in liver of P6 and P7 (Supplementary Figure S2). CLDN1, together with other claudins, is integral to tight-junction structure. TJP2 binds to the cytoplasmic C terminus of CLDN1, linking it to the actin cytoskeleton. CLDN1 deficiency-associated disease includes a syndromic form of neonatal sclerosing cholangitis.²⁰

The mouse-deafness model of *USP53* mutation, as described, does not include hepatobiliary disease,⁹ and thus morphologic study of *Usp53*-mutated mouse liver has not been undertaken. In the mouse inner ear, however, although cochlear hair-cell loss was accelerated, on ultrastructural study no tight-junction abnormalities were found.⁹ By contrast, liver from patients P3 and P4 on transmission electron microscopy displayed abnormalities in tight junctions, with elongation, that resemble those in *TJP2* disease.^{18,19} Although icterus resolved in our patients, *USP53* disease appears unlikely to be entirely bland; light microscopy of liver-biopsy material found, along with intralobular cholestasis, fibrosis with parenchymal nodularity (cirrhotic transformation) in 4 patients aged \approx 10mo (P3, P4, P6, and P7). Severe *TJP2* disease predisposes to hepatocellular malignancy.^{21,22} Monitoring of *USP53* disease patients for malignancy may be in order.

Our observations also suggest diversity in disease severity among *USP53* patients. Of the 3 reported Saudi children who harbored homozygous *USP53* variants predicted to abolish expression, one underwent liver transplantation aged 6y.² However, among our 6 patients available for follow-up, although patients P1, P2, P4, and P5 harbor 2 copies of *USP53* variants predicted to abolish expression completely, under traditional management with UDCA and / or cholestyramine all 6 retain their native livers, with normalized serum bilirubin levels in all. Indeed, in 3 all values for biomarkers of hepatobiliary disease have normalized (Table 2).

This diversity extends to hearing. Two Saudi *USP53*-disease patients, both female, had late-onset deafness (aged 14y and 9y),² whilst our patient P6 was identified as deaf from birth. The third Saudi *USP53*-disease patient, however, a male aged 3y when described, was not deaf. Our other patients, the oldest now aged 5y, have no manifestation of hearing loss. However, they must be monitored for hearing loss and kept from further injury such as that imposed by aminoglycoside antibiotics.

We note with interest a higher rate of heterozygosity for *USP53* PPVs in our “other-liver-disease” cohort (3/168) than that in our “non-liver-disease” control cohort (11/2000). The difference is of marginal statistical significance at $p=0.088$ (Supplementary Table S3). *USP53* mutation in the heterozygous state may increase the penetrance or severity of liver disease that cannot be ascribed to *USP53* disease alone. In the 7 patients with *USP53* disease, heterozygous mutations in other cholestasis-associated genes such as *TJP2*, *MYO5B*, and *VPS33B* were discovered in P2, P5, and P6 respectively (Supplementary Table S1). How they contribute to the diversity and severity of the *USP53* disease warrants further investigation.

That commercially available antibodies against *USP53* failed, in our hands, to mark formalin-fixed, paraffin-embedded liver in a reproducible manner is to be regretted; this constitutes a deficiency in our study. The absence of histological data in some patients is also a limit of the retrospective study.

Conclusion

Our identification of 7 patients with biallelic pathogenic or likely pathogenic variants in *USP53*, in

association with low-GGT cholestasis, together with light-microscopy findings and ultrastructural findings on liver biopsy, extends a preliminary report of *USP53* mutation in intrahepatic cholestasis. Our observations further suggest that *USP53* mutation may generate a partial phenocopy of *TJP2* disease in both the liver and the ear.

(2452 words)

Acknowledgements

We thank the study families for their enthusiastic participation. We thank Dr. Bo Duan (Department of Otolaryngology Head and Neck Surgery, Children's Hospital of Fudan University) for helping to interpret auditory test results.

Data availability statement

All data relevant to the study are included in the article or uploaded as supplementary information. We have submitted our list of variations to Clinvar. The URLs are <https://www.ncbi.nlm.nih.gov/clinvar/submitters/507193>.

References

1. Lane E, Murray KF. Neonatal cholestasis. *Pediatr Clin North Am*. 2017;64(3):621-639.
2. Maddirevula S, Alhebbi H, Alqahtani A, et al. Identification of novel loci for pediatric cholestatic liver disease defined by KIF12, PPM1F, USP53, LSR, and WDR83OS pathogenic variants. *Genet Med*. 2019;21(5):1164-1172.
3. Qiu YL, Gong JY, Feng JY, et al. Defects in myosin VB are associated with a spectrum of previously undiagnosed low gamma-glutamyltransferase cholestasis. *Hepatology*. 2017;65(5):1655-1669.
4. Togawa T, Sugiura T, Ito K, et al. Molecular genetic dissection and neonatal/infantile intrahepatic cholestasis using targeted next-generation sequencing. *J Pediatr*. 2016;171:171-177 e171-174.
5. Wang NL, Lu YL, Zhang P, et al. A specially designed multi-gene panel facilitates genetic diagnosis in children with intrahepatic cholestasis: simultaneous test of known large insertions/deletions. *Plos One*. 2016;11(10):e0164058.

6. Schwarz JM, Cooper DN, Schuelke M, Seelow D. MutationTaster2: mutation prediction for the deep-sequencing age. *Nat Methods*. 2014;11(4):361-362.
7. Adzhubei I, Jordan DM, Sunyaev SR. Predicting functional effect of human missense mutations using PolyPhen-2. *Curr Protoc Hum Genet*. 2013;Chapter 7:Unit7 20.
8. Kumar P, Henikoff S, Ng PC. Predicting the effects of coding non-synonymous variants on protein function using the SIFT algorithm. *Nat Protoc*. 2009;4(7):1073-1081.
9. Kazmierczak M, Harris SL, Kazmierczak P, et al. Progressive hearing loss in mice carrying a mutation in *Usp53*. *J Neurosci*. 2015;35(47):15582-15598.
10. Girard M, Lacaille F, Verkarre V, et al. MYO5B and bile salt export pump contribute to cholestatic liver disorder in microvillous inclusion disease. *Hepatology*. 2014;60(1):301-310.
11. American Academy of Pediatrics JCoIH. Year 2007 position statement: Principles and guidelines for early hearing detection and intervention programs. *Pediatrics*. 2007;120(4):898-921.
12. Wroblewska-Seniuk KE, Dabrowski P, Szyfter W, Mazela J. Universal newborn hearing screening: methods and results, obstacles, and benefits. *Pediatr Res*. 2017;81(3):415-422.
13. Richards S, Aziz N, Bale S, et al. Standards and guidelines for the interpretation of sequence variants: a joint consensus recommendation of the American College of Medical Genetics and Genomics and the Association for Molecular Pathology. *Genet Med*. 2015;17(5):405-424.
14. Quesada V, Díaz-Perales A, Gutiérrez-Fernández A, Garabaya C, Cal S., López-Otín C. Cloning and enzymatic analysis of 22 novel human ubiquitin-specific proteases. *Biochem Biophys Res Commun*. 2004;314(1):54-62.
15. Walsh T, Pierce SB, Lenz DR, et al. Genomic duplication and overexpression of *TJP2/ZO-2* leads to altered expression of apoptosis genes in progressive nonsyndromic hearing loss DFNA51. *Am J Hum Genet*. 2010;87(1):101-109.
16. Wang HY, Zhao YL, Liu Q, et al. Identification of two disease-causing genes *TJP2* and *GJB2* in a Chinese family with unconditional autosomal dominant nonsyndromic hereditary hearing impairment. *Chin Med J (Engl)*. 2015;128(24):3345-3351.
17. Zou S, Mei X, Yang W, Zhu R, Yang T, Hu H. Whole-exome sequencing identifies rare pathogenic and candidate variants in sporadic Chinese Han deaf patients. *Clin Genet*. 2019;1-5.

18. Carlton VE, Harris BZ, Puffenberger EG, et al. Complex inheritance of familial hypercholanemia with associated mutations in TJP2 and BAAT. *Nat Genet.* 2003;34(1):91-96.
19. Sambrotta M, Strautnieks S, Papouli E, et al. Mutations in TJP2 cause progressive cholestatic liver disease. *Nat Genet.* 2014;46(4):326-328.
20. Hadj-Rabia S, Baala L, Vabres P, et al. Claudin-1 gene mutations in neonatal sclerosing cholangitis associated with Ichthyosis: A tight junction disease. *Gastroenterology.* 2004;127(5):1386-1390.
21. Zhou S, Hertel PM, Finegold MJ, et al. Hepatocellular carcinoma associated with tight-junction protein 2 deficiency. *Hepatology.* 2015;62(6):1914-1916.
22. Vij M, Shanmugam NP, Reddy MS, Sankaranarayanan S, Rela M. Paediatric hepatocellular carcinoma in tight junction protein 2 (TJP2) deficiency. *Virchows Arch.* 2017;471(5):679-683.

Figure legends

Figure 1. Pedigrees of 7 families in which a child had intrahepatic cholestasis associated with *USP53* variants.

Seven patients with homozygous or compound heterozygous variants in *USP53* were identified (all by exome sequencing). Variants in each family were confirmed by Sanger sequencing (NA, sample not available). Hyphen, wild-type status. Siblings of P2: Clinically well, not genotyped. All patients of Han descent bilaterally except P1 (father, Manchu ethnicity).

Figure 2. Histological findings in *USP53* patients P3, P4, P6, and P7 and in a TJP2 patient.

In *USP53* patients, note disarrayed lobule; giant-cell change, circled, and rosetting of hepatocytes with canalicular cholestasis, white arrow (P3, upper panel, original magnification 200x; pericellular fibrosis, signs of nodularity and hepatocellular rosetting centered on dilated bile canaliculi with bile plugs, white arrow (P4, upper panel, original magnification 200x); disarray with canalicular cholestasis, black arrow (P6, upper panel, original magnification 400x); disarray and canalicular cholestasis (P7, upper panel, original magnification 400x); bridging fibrosis and

nodularity (P3, lower panel, original magnification 100x); interstitial fibrosis (P4, lower panel, original magnification 100x); cirrhosis (P6, lower panel, original magnification 100x); portal-tract fibrosis and inflammation, white arrow, with intralobular cholestasis (P7, lower panel, original magnification 200x). In a TJP2 patient, note bridging fibrosis and nodularity (S1, original magnification 100x); disarray with hepatocyte multinucleation, white arrow (S2, original magnification 200x); slight portal-tract inflammation, white arrow, with intralobular cholestasis (S3, original magnification 200x); and hepatocellular rosetting with canalicular cholestasis, white arrow (S4, original magnification 400x). Liver-biopsy material at presentation, all images; lower panels, P3 and P4, Gömöri reticulin stain, all others hematoxylin / eosin.

Figure 3. Transmission electron micrographs of tight junction structure in liver biopsy specimens.

All four panels show tight-junction complexes between adjacent hepatocytes and biliary canaliculi. In each panel, a red asterisk indicates the canalicular space. Panels a and b are from liver biopsy specimens obtained from P3 and P4, respectively. Panel c is from a patient with *ABCB11* disease and panel d from a patient with *ATP8B1* disease. All biopsy specimens were primarily fixed at bedside for transmission electron microscopy. Tight junctions appear to extend deeper into the paracellular, or lateral, space in the *USP53*-mutated patients than in the comparison patients, with diminution of the most electron-dense part of the zona occludens (shown with arrows). In all panels, the scale bar=1000 nm; osmium tetroxide / uranyl acetate / lead citrate.

Table 1. Predicted pathogenicities of 10 *USP53* variations

| cDNA change (NM_019050.2) | predicted effects (NP_061923.2) | ExAC ^a (hom / het / total) [†] | 1000G ^b | <i>In silico</i> pathogenicity predictions (SIFT ^c / PPH2 ^d / Mut ^e / BDGP ^f / HSF ^g) |
|------------------------------|------------------------------------|---|--------------------|--|
| c.169C>T | p.Arg57Ter | — | — | NA / NA / disease-causing / ND / ND |
| c.297G>T | p.Arg99Ser | — | — | damaging / probably damaging / disease-causing / N / new donor site |
| c.395A>G | p.His132Arg | — | — | damaging / probably damaging / disease-causing / N / N |
| c.569+2T>C | splicing | — | — | NA / NA / disease-causing / donor lost / new ESS site |
| c.581delA | p.Arg195GlufsTer38 | — | — | NA / NA / disease-causing / ND / ND |
| c.831_832insAG | p.Val279GlufsTer16 | — | — | NA / NA / disease-causing / ND / ND |
| c.878G>T | p.Gly293Val | — | — | damaging / probably damaging / disease-causing / donor lost / new ESS site |
| c.1012C>T | p.Arg338Ter | 0 / 2 / 60263 | — | NA / NA / disease-causing / ND / ND |
| c.1426C>T | p.Arg476Ter | 0 / 19 / 57877 | — | NA / NA / disease-causing / ND / ND |
| c.1558C>T | p.Arg520Ter | — | — | NA / NA / disease-causing / ND / ND |

Table 2. Clinical and biomarker features and outcomes for 7 patients

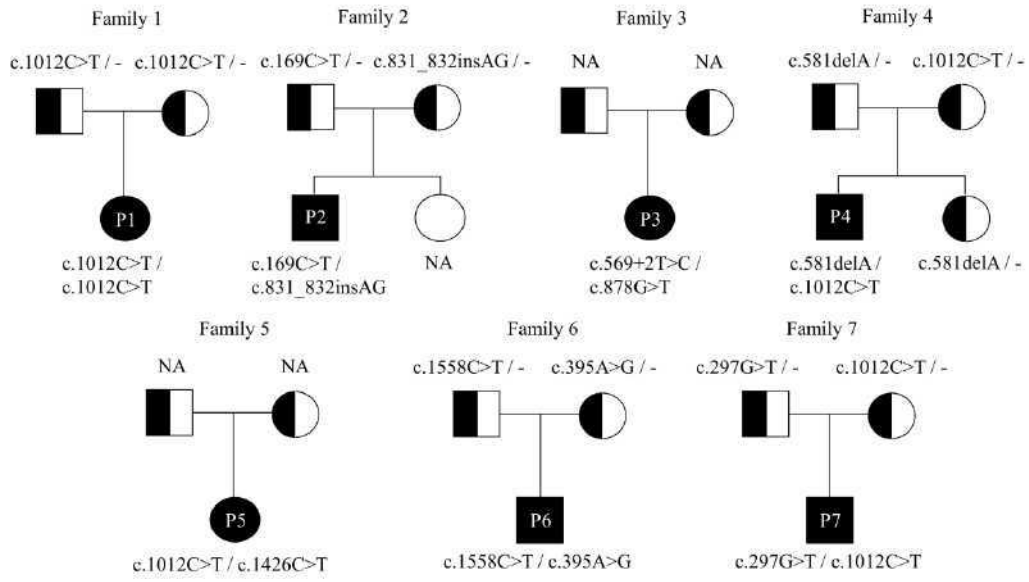
| Patient | Sex / age ^a | Age ^b | TB / DB | ALT / AST | ALP / GGT | UDCA / cholestyramine ^c | Outcome after Medical treatment |
|---------|------------------------|------------------|------------------|------------------|------------------|------------------------------------|---|
| P1 | F / 3d | 12mo21d | 23 / 19 | 184 / 215 | 330 / 23 | UDCA and cholestyramine | Alive with native liver at 2y. |
| | | 18mo | 11 / 3 | 60 / 58 | 1259 / 19 | Stop medicine | |
| P2 | M / 2d | 4mo15d | 90 / 65 | 70 / 71 | 548 / 72 | UDCA | Alive with native liver at 3y6mo. |
| | | 1y6mo | 11 / 6 | 263 / 141 | 377 / 23 | Cholestyramine | |
| | | 3y6mo | 8 / 2 | 33 / 32 | 332 / 26 | Stop medicine | |
| P3 | F / 6mo | 8mo25d | 212 / 159 | 103 / 121 | - / 34 | UDCA | Alive with native liver at 5y. |
| | | 12mo1d | 6 / 4 | 74 / 85 | 305 / 20 | Unknown | |
| P4 | M / 5mo | 9mo25d | 308 / 167 | 32 / 84 | 636 / 39 | UDCA and cholestyramine | Alive with native liver at 17mo. |
| | | 17mo | 11 / 4 | 49 / 72 | - / 16 | cholestyramine | |
| P5 | F / 1mo | 4mo18d | 275 / 216 | 28 / 51 | 543 / 40 | UDCA | Lost to follow-up. |
| | | 8mo13d | 33 / 27 | 141 / 87 | 626 / 18 | UDCA | |
| P6 | M / 5mo | 6mo | 85 / 72 | 26 / 41 | 342 / 27 | UDCA and cholestyramine | Alive with native liver at 1y3mo; cochlear implant at 1y3mo. |
| | | 1y1mo | 6 / 3 | 27 / 54 | 365 / 15 | cholestyramine | |
| P7 | M / 7mo | 8mo | 153 / 137 | 18 / 225 | 283 / 22 | UDCA and cholestyramine | Alive with native liver at 1y1mo. |
| | | 1y1mo | 18 / 13 | 63 / 89 | 254 / 30 | UDCA and cholestyramine | |

a, b: Age of jaundice onset and age of sampling; c, dose for UDCA was 20 mg / kg / day and dose for cholestyramine was 1 ~ 2g once a day.

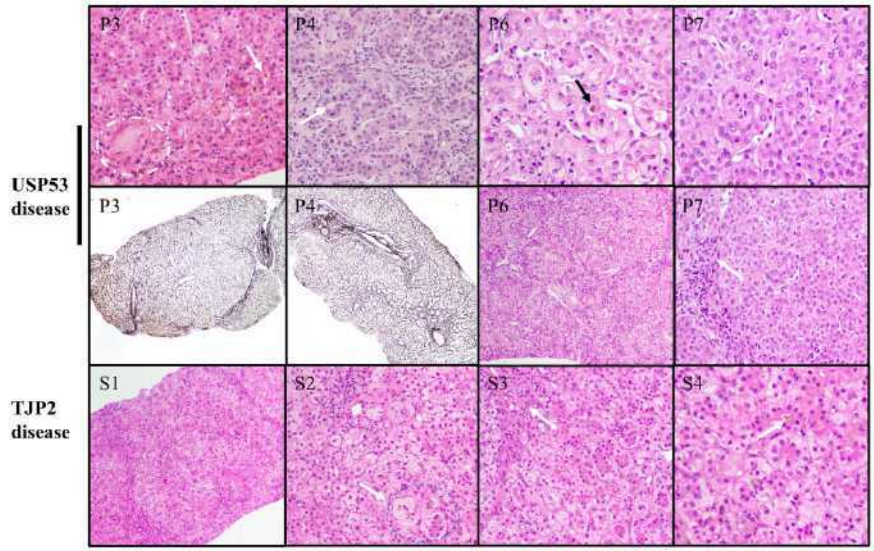
d, days; mo, months; y, years; -, not available. Biomarker values in **boldface** are abnormal.

TB, total bilirubin; DB, direct bilirubin; ALT, alanine aminotransferase; AST, aspartate aminotransferase; ALP, alkaline phosphatase; GGT, gamma-glutamyl transferase; TBA, total bile acids.

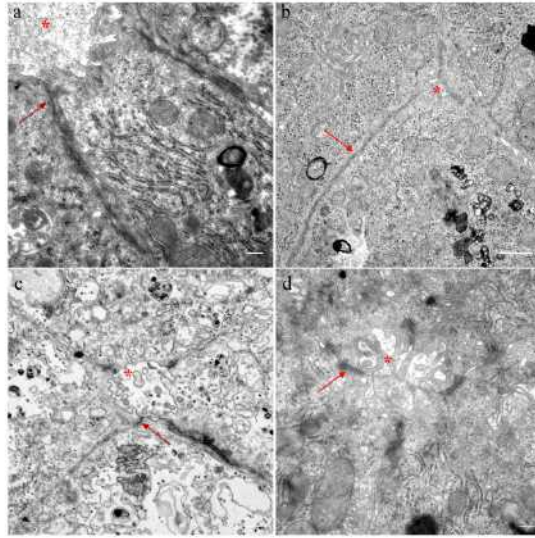
Reference data (expected values) for children: TB 5.1-20 $\mu\text{mol} / \text{L}$, DB 0-6 $\mu\text{mol} / \text{L}$, ALT 0-40 IU / L, AST 15-60 IU / L, ALP 42-383 IU / L; GGT 7-50 IU / L; TBA 0-10 $\mu\text{mol} / \text{L}$



liv_14422_f1.tif



liv_14422_f2.tif



liv_14422_f3.tif